《原子核物理评论》
www.npr.ac.cn Nuclear Physics Review
Started in 1984

因果率限制下重子三体力对K介子凝聚状态方程的影响

武藤巧

Effects of Three-Baryon Forces Constrained by Causality Condition on the Equation of State with Kaon Condensation

MUTO Takumi

在线阅读 View online: https://doi.org/10.11804/NuclPhysRev.41.QCS2023.08

引用格式:
武藤巧. 因果率限制下重子三体力对K介子凝聚状态方程的影响[J]. 原子核物理评论, 2024, 41(3):828-833. doi: 10.11804/NuclPhysRev.41.QCS2023.08
MUTO Takumi. Effects of Three-Baryon Forces Constrained by Causality Condition on the Equation of State with Kaon Condensation[J]. Nuclear Physics Review, 2024, 41(3):828-833. doi: 10.11804/NuclPhysRev.41.QCS2023.08

您可能感兴趣的其他文章

Articles you may be interested in

致密物质状态方程：中子星与奇异星
Dense Matter Equation of State: Neutron Star and Strange Star
原子核物理评论. 2019, 36(1): 1-36 https://doi.org/10.11804/NuclPhysRev.36.01.001

利用两π介子HBT关联约束重离子碰撞中高密核物质的状态方程
The High-density Equation of State in Heavy-ion Collisions: Constraints from Two-pion HBT Correlation
原子核物理评论. 2024, 41(1): 522-529 https://doi.org/10.11804/NuclPhysRev.41.2023CNPC16

中子星状态方程的天文和实验室研究
Astrophysical and Laboratory Studies on the Equation of State of Neutron Stars
原子核物理评论. 2024, 41(1): 308-317 https://doi.org/10.11804/NuclPhysRev.41.2023CNPC36

利用深度学习方法研究核物质状态方程
Using Deep Learning to Study the Equation of State of Nuclear Matter
原子核物理评论. 2020, 37(4): 825-832 https://doi.org/10.11804/NuclPhysRev.37.2020017

中子星可观测量与不同密度段核物质状态方程的关联
Correlation Between Neutron Star Observation and Equation of State of Nuclear Matter at Different Densities
原子核物理评论. 2021, 38(2): 123-128 https://doi.org/10.11804/NuclPhysRev.38.2021019

核物质和中子星物质的相对论第一性原理研究
Relativistic *ab initio* Studies for Nuclear Matter and Neutron Star Matter
原子核物理评论. 2024, 41(1): 299-307 https://doi.org/10.11804/NuclPhysRev.41.2023CNPC07

第 41 卷 第 3 期
2024 年 9 月
原 子 核 物 理 评 论
Nuclear Physics Review
Vol. 41, No. 3
Sep., 2024

Article ID: 1007-4627(2024)03–0828–06

Effects of Three-Baryon Forces Constrained by Causality Condition on the Equation of State with Kaon Condensation

MUTO Takumi

(*Physics Division, Education Center, Chiba Institute of Technology, Narashino, Chiba 275-0023, Japan*)

Abstract: Possibility of kaon-condensed phase in hyperon-mixed matter is considered as high-density multi-strangeness system, which may be realized in neutron stars. The interaction model is based on chiral symmetry for kaon-baryon and kaon-kaon interactions, being combined with the relativistic mean-field theory for two-body baryon-baryon (B-B) interaction. In addition, the Lorentz invariant forms of many-baryon repulsive force (MBR) and three-nucleon attractive force (TNA) are phenomenologically introduced, where unknown parameters are fixed to satisfy the saturation properties of symmetric nuclear matter and the causality condition that the sound velocity should be less than the speed of light. It is shown that the equation of state with kaon condensation in hyperon-mixed matter is stiff enough to be consistent with recent observations of massive neutron stars.

Key words: dense hadronic matter; kaon condensation; equation of state; causality

CLC number: O571.6 **Document code:** A

DOI: 10.11804/NuclPhysRev.41.QCS2023.08 **CSTR:** 32260.14.NuclPhysRev.41.QCS2023.08

0 Introduction

Multi-strangeness phases in dense hadronic matter have been one of important topics of hadron physics. Kaon condensation (KC), Bose-Einstein condensation as a macroscopic appearance of strangeness, has been attracting much interest, and the characteristic features and its possible existence have been extensively studied from both theoretical and observational or experimental viewpoint[1−6]. In neutron stars, hyperons (Y) ($Y = \Lambda$, Σ^-, Ξ^- $\cdots$) may be mixed in the ground state of hadronic matter. Both KC and hyperon-mixed matter have common features: 1) Softening of the equation of state (EOS) leading to reduced maximum mass of neutron star and its radius, and 2) rapid cooling mechanisms via neutrino emissions, affecting thermal evolution of neutron stars. These KC and Y-mixed phases are likely to coexist in inner cores of neutron stars. We call the possible coexistent phase with KC and Y-mixed matter as ($Y+K$) phase. Both KC and Y-mixing lead to significant softening of the EOS as a consequence of the combined effects of decreasing energy by the s-wave K-baryon (B) attraction and avoiding the N-N repulsion at high densities by Y-mixing[7]. The maximum mass of neutron stars with the (Y+K) phase within the two-body B-B interaction only becomes too low to be compatible with observations of massive neutron stars[8−13].

In the case of hyperon-mixed matter, the problem originating from dramatic softening of the EOS has been called "hyperon puzzle". To resolve the hyperon puzzle, the necessity of introducing the universal three-baryon repulsion (UTBR) among hyperons and nucleons (YYY, YYN, YNN) as well as three-nucleon (NNN) force was pointed out[7, 14−15]. For the ($Y+K$) phase, we have introduced the UTBR, which has been derived based on the string-junction model-2 (SJM2) by Tamagaki[14−15], and we have shown that the UTBR appropriately stiffen the EOS, consistent with recent observations of massive neutron stars. However, it has been shown that for some parameter sets with the slope L of the symmetry energy, the EOS including the SJM2 as the UTBR violates the causality condition, *i.e.*, the sound velocity v_s exceeds the speed of light c, beyond certain densities. Specifically, for L = 60 MeV and 65 MeV, the causality condition is violated before a neutron star gravitational mass reaches the maximum mass[16−17].

In this work, we assume a Lorentz-scalar form for UTBR as a necessary but not sufficient condition so as to satisfy the causality condition. We obtain a sufficient EOS for the (Y+K) phase, which meets the saturation properties of symmetric nuclear matter (SNM) and also is consistent with recent observations of massive neutron stars. We clarify how the causality condition affects stiffness of the EOS with the (Y+K) phase. Modification of properties of the

Received date: 12 Dec. 2023; **Revised date:** 18 Mar. 2024

Biography: MUTO Takumi(1960−), male(Japanese), Shizuoka Prefecture, Ph.D./Professor, working on nuclear physics;
E-mail: takumi.muto@it-chiba.ac.jp

(Y+K) phase (onset density of KC, the EOS at high densities $\cdots$) is also discussed.

1　Interaction model for the (Y+K) phase

1.1　K - B and K - K interactions in chiral symmetry

The (Y+K) phase is composed of kaon condensates and hyperon-mixed baryonic matter together with leptons, being kept in beta equilibrium, charge neutrality, and baryon number conservation. In the following, we simply take into account protons, neutrons, Λ, Σ^-, and Ξ^- hyperons for baryons and electrons and muons for leptons.

We base our model for K-B and K-K interactions upon the effective chiral $\mathrm{SU(3)}_L\times\mathrm{SU(3)}_R$ Lagrangian[1, 16–17].

$$
\begin{aligned}
\mathcal{L}_{K,B} =& \frac{1}{4}f^2\ \mathrm{Tr}(\partial^\mu U^\dagger\partial_\mu U)+\\
&\frac{1}{2}f^2\Lambda_{\chi\mathrm{SB}}(\mathrm{Tr}M(U-1)+\mathrm{h.c.})+\\
&\mathrm{Tr}\overline{\Psi}(\mathrm{i}\gamma^\mu\partial_\mu-M_\mathrm{B})\Psi+\mathrm{Tr}\overline{\Psi}\gamma^\mu[V_\mu,\Psi]+\\
&D\mathrm{Tr}\overline{\Psi}\gamma^\mu\gamma^5\{A_\mu,\Psi\}+F\mathrm{Tr}\overline{\Psi}\gamma^\mu\gamma^5[A_\mu,\Psi]+\\
&a_1\mathrm{Tr}\overline{\Psi}(\xi M^\dagger\xi+\mathrm{h.c.})\Psi+a_2\mathrm{Tr}\overline{\Psi}\Psi(\xi M^\dagger\xi+\mathrm{h.c.})+\\
&a_3(\mathrm{Tr}MU+\mathrm{h.c.})\mathrm{Tr}\overline{\Psi}\Psi\ ,
\end{aligned}
\tag{1}
$$

where the first and second terms are kinetic and mass terms of the nonlinear meson fields, $U=\exp(2\mathrm{i}\pi_aT_a/f)$ with π_a ($a=1\sim 8$) being the octet mesons, T_a the flavor SU(3) generator, f (= 93 MeV) the meson decay constant, $\Lambda_{\chi SB}$ ~1 GeV the chiral-symmetry breaking scale, and M (= $\mathrm{diag}(m_u,m_d,m_s)$) the quark mass matrix. The third term in Eq. (1) is kinetic and mass terms of the octet baryons Ψ with M_B being the spontaneously broken baryon mass. The fourth term represents the s-wave K-B vector interaction with $V_\mu\equiv\frac{\mathrm{i}}{2}(\xi^\dagger\partial_\mu\xi+\xi\partial_\mu\xi^\dagger)$ being the vector current for meson ξ (= $U^{1/2}$) field. This term corresponding to the Tomozawa-Weinberg term plays a role of one of the main driving force for KC. The fifth and sixth terms (F and D terms), with $A_\mu\equiv\frac{\mathrm{i}}{2}(\xi^\dagger\partial_\mu\xi-\xi\partial_\mu\xi^\dagger)$ being the axial-vector current for meson, lead to the p-wave K-B interactions, which we simply neglect here since only the s-wave condensation is considered. The last three terms with the coefficients $a_1\sim a_3$ in Eq. (1) give another driving forces for KC, simulated by the K-B sigma terms ($\Sigma_{Kb}\equiv\frac{1}{2}(m_u+m_s)\langle b|(\bar{u}u+\bar{s}s)|b\rangle$) ($b=p,n,\Lambda,\Sigma^-,\Xi^-$), which break chiral symmetry explicitly. Throughout this paper, we consider only the $K^\pm$ [= $(\pi_4\mp\mathrm{i}\pi_5)/\sqrt{2}$] for π_a and nucleons (p , n), and Λ, Σ^-, Ξ^- hyperons for Ψ.

The meson field U, ξ, and the baryon field Ψ are transformed by chiral transformation as $U\to U'=LUR^\dagger$, $\xi\to\xi'=L\xi h^\dagger=h\xi R^\dagger$, $\Psi\to\Psi'=h\Psi h^\dagger$, $\overline{\Psi}\to\overline{\Psi}'=h\overline{\Psi}h^\dagger$. with $R\in\mathrm{SU(3)}_R$, $L\in\mathrm{SU(3)}_L$, and $h=\sqrt{LUR^\dagger}R\sqrt{U^\dagger}\in\mathrm{SU(3)}_V$.

The condensed kaon field is assumed to be spatially uniform with spatial momentum $k=0$ and represented classically as

$$
K^\pm=\frac{f}{\sqrt{2}}\theta\exp(\pm\mathrm{i}\mu_K t)\ ,
\tag{2}
$$

where θ the chiral angle, and μ_K is the K^- chemical potential.

1.2　B - B interaction in the minimal RMF

We adopt the RMF model for two-body B - B interaction mediated by the scalar (σ, σ^*) mesons and vector (ω, ρ, ϕ) mesons, discarding the *nonlinear* self-interacting σ,ω, or $\omega-\rho$ meson-coupling potentials[18]. We call this model a minimal RMF (MRMF)[16].

1.3　Lorentz-invariant forms for universal three-baryon repulsion

Since a contribution from many-baryon forces to the energy density, $\mathcal{E}$ (MBR), is of Lorentz scalar in the RMF, we assume that a phenomenological form of the $\mathcal{E}$ (MBR) is represented as a sum of power functions with m,n (= 0, 1, $\cdots$) in terms of baryon scalar density ρ_B^s (= $\langle\overline{\Psi}\Psi\rangle$) and product of baryon current density, $\langle\overline{\Psi}\gamma^\mu\Psi\rangle\cdot\langle\overline{\Psi}\gamma_\mu\Psi\rangle$. In the following, the form with simple choice of m, n is utilized as

$$
\begin{aligned}
\mathcal{E}\,(\mathrm{MBR}) &= \sum_{m,n}c_{m,n}(\mathrm{Tr}\bar{\psi}\psi)^m\left(\mathrm{Tr}(\bar{\psi}\gamma^\mu\psi\cdot\bar{\psi}\gamma_\mu\psi)\right)^n\\
&\to\mathcal{E}\,(\mathrm{CovMBR3})+\mathcal{E}\,(\mathrm{CovMBR4})
\end{aligned}
\tag{3}
$$

with

$$
\mathcal{E}\,(\mathrm{CovMBR3})=c_3\rho_\mathrm{B}^s\rho_\mathrm{B}^2\ ,
\tag{4a}
$$

$$
\begin{aligned}
\mathcal{E}\,(\mathrm{CovMBR4}) &= c_4\rho_\mathrm{B}^2[1-\exp(-\eta\rho_\mathrm{B}^2)]\\
&= c_4\rho_\mathrm{B}^2\left(\eta\rho_\mathrm{B}^2-\frac{1}{2!}\eta^2\rho_\mathrm{B}^4+\cdots\right)\ ,
\end{aligned}
\tag{4b}
$$

where only the time component ($\mu=0$) of the baryon number current, *i.e.*, ρ_B , is retained for the ground state matter, and many-baryon forces participating more than three baryons are imitated through the exponential factor $\propto\exp(-\eta\rho_\mathrm{B}^2)$, as seen from the second line on the r. h. s. of Eq. (4b). In Eq. (4a), the baryon scalar density $\rho_\mathrm{B}^s\left(=\sum_{b=p,n,\Lambda,\Sigma^-,\Xi^-}\rho_b^s\right)$ isgivenwith $\rho_b^s=\frac{2}{(2\pi)^3}\int_{|\boldsymbol{p}|\leqslant p_F(b)}\mathrm{d}^3|\boldsymbol{p}|\frac{\widetilde{M}_b^*}{(|\boldsymbol{p}|^2+\widetilde{M}_b^{*2})^{1/2}}$, where $\widetilde{M}_b^*$ is the effective baryon mass in KC, $\widetilde{M}_b^*\equiv M_b-g_{\sigma b}\sigma-g_{\sigma^*b}\sigma^*-\Sigma_{Kb}(1-\cos\theta)$. The energy density expression for MBR, Eq. (3), is invariant under chiral transformation, $\Psi\to\Psi'=h\Psi h^\dagger$, $\overline{\Psi}\to\overline{\Psi}'=h\overline{\Psi}h^\dagger$.

The attractive contribution from the three-nucleon interaction (TNA) is adopted as the same expression as Lagaris and Pandharipande (LP1981)[19], while the relevant parameters η_a, γ_a in the TNA are modified according to our model.

1.4 Energy expression for the (*Y*+*K*) phase

The energy density expression $\mathcal{E}$ for the (*Y*+*K*) phase is given as

$$\begin{aligned}\mathcal{E}=&\frac{1}{2}(\mu_K f\sin\theta)^2+f^2m_K^2(1-\cos\theta)+\\&\sum_{b=p,n,\Lambda,\Sigma^-,\Xi^-}\frac{2}{(2\pi)^3}\int_{|\boldsymbol{p}|\leqslant p_F(b)}\mathrm{d}^3|\boldsymbol{p}|(|\boldsymbol{p}|^2+\widetilde{M}_b^{*2})^{1/2}+\\&\frac{1}{2}\left(m_\sigma^2\sigma^2+m_{\sigma^*}^2\sigma^{*2}\right)+\frac{1}{2}\left(m_\omega^2\omega_0^2+m_\rho^2R_0^2+m_\phi^2\phi_0^2\right)+\\&c_3\rho_B^s\rho_B{}^2+c_4\rho_B^2[1-\exp(-\eta\rho_B^2)]+\\&\gamma_a\rho_B^3e^{-\eta_a\rho_B}\{3-2(1-2x_p)^2\}+\mathcal{E}_e+\mathcal{E}_\mu\ ,\end{aligned}\tag{5}$$

where the first and second terms are kinetic and mass terms of KC, respectively. The third term is the kinetic energy density for baryons b. The σ and σ^* ($\sim\langle\bar{s}s\rangle$) in the fourth term are the contribution from the scalar mean fields, and the ω_0, R_0 [$\equiv R_0^3$, which is assumed to have only the third component of isospin], and $\phi_0\sim\langle\bar{s}\gamma^0 s\rangle$) in the fifth term are from the time-components of the vector mean fields. They are taken to be uniform to describe the ground state of the (Y+K) phase. The meson masses are set to be m_σ = 400 MeV, m_{σ^*} = 975 MeV, m_ω = 783 MeV, m_ρ = 769 MeV, and m_ϕ = 1 020 MeV. The sixth and seventh terms are from MBR [(3)], and the eighth term from the TNA. The last two terms are the free leptonic (e^- and μ^-) energy densities:

$$\mathcal{E}_e\simeq\mu_e^4/(4\pi^2)\ ,\tag{6}$$

$$\begin{aligned}\mathcal{E}_\mu=&\frac{2}{(2\pi)^3}\int_{|\boldsymbol{p}|\leqslant p_F(\mu^-)}\mathrm{d}^3|\boldsymbol{p}|(|\boldsymbol{p}|^2+m_\mu^2)^{1/2}\\=&\frac{m_\mu^4}{8\pi^2}\left[r(1+2r^2)\sqrt{r^2+1}-\log(r+\sqrt{r^2+1})\right]\end{aligned}\tag{7}$$

with $r\equiv p_F(\mu^-)/m_\mu$, where

$$p_F(\mu^-)\equiv\sqrt{\mu^2-m_\mu^2}\cdot\Theta(\mu^2-m_\mu^2)$$

is the muon Fermi momentum with the charge chemical potential μ and the step function $\Theta(x)$. It is to be noted that the electrons are ultra-relativistic, since the typical electron momentum is much larger than the electron rest mass in the core of neutron stars.

The effective energy density is constructed by taking into account charge conservation and baryon number conservations as $\mathcal{E}^{\rm eff}\equiv\mathcal{E}+\mu\rho_Q+\nu\rho_B$, where μ is the charge chemicl potential, ρ_Q the charge density, ν the baryon numer chemical potential. The classical field equation for KC reads from $\partial\mathcal{E}^{\rm eff}/\partial\theta=0$:

$$\begin{aligned}&\mu_K^2\cos\theta-m_K^2+\frac{1}{f^2}\sum_{b=p,n,\Lambda,\Xi^-,\Sigma^-}\Sigma_{Kb}\left[\rho_b^s+c_3\rho_B^2\bar{I}(p_F(b))\right]+\\&2\mu_K X_0=0\ ,\end{aligned}\tag{8}$$

where $\bar{I}(p_F(b))\equiv\int_0^{p_F(b)}\mathrm{d}|\boldsymbol{p}|\frac{|\boldsymbol{p}|^4}{\sqrt{|\boldsymbol{p}|^2+\widetilde{M}_b^{*2}}}$, and $X_0\equiv\frac{1}{2f^2}\left(\rho_p+\frac{1}{2}\rho_n-\frac{1}{2}\rho_{\Sigma^-}-\rho_{\Xi^-}\right)$, which has an attractive contribution from the s-wave K-B vector interaction for $X_0>0$. From Eq. (8) one can see that the s-wave K-B attractive scalar interaction simulated by the Kb sigma terms, Σ_{Kb}, is enhanced by the introduction of CovMBR3 through the θ-dependence of the baryon scalar density ρ_B^s in the $\mathcal{E}$ (CovMBR3) [Eq. (4)].

The ground state energy for the ($Y+K$) phase is obtained under the charge neutrality condition, $\partial\mathcal{E}^{\rm eff}/\partial\mu=\rho_Q=\rho_p-\rho_{\Sigma^-}-\rho_{\Xi^-}-\rho_{K^-}-\rho_e-\rho_\mu=0$, baryon number conservation, $\partial\mathcal{E}^{\rm eff}/\partial\nu=\rho_p+\rho_n+\rho_\Lambda+\rho_{\Sigma^-}+\rho_{\Xi^-}=\rho_B$, and β-equilibrium conditions, $n\rightleftharpoons p+K^-$, $n\rightleftharpoons p+e^-(+\bar{\nu}_e)$, $n+e^-\rightleftharpoons\Sigma^-(+\nu_e)$, $\Lambda+e^-\rightleftharpoons\Xi^-(+\nu_e)$, $n\rightleftharpoons\Lambda(+\nu_e\bar{\nu}_e)$, and those involved in muons in place of e^- if muons are present.

1.5 Saturation properties in SNM and parameters

In order to determine the meson-nucleon coupling constants, $g_{\sigma N}$, $g_{\omega N}$, $g_{\rho N}$, and the σ, ω mean fields, $\langle\sigma\rangle_0$, $\langle\omega_0\rangle_0$, and parameters in TNA, η_a, γ_a, we impose the saturation properties of the symmetric nuclear matter (SNM), *i.e.*, the saturation density ρ_0 = 0.16 fm^{-3}, binding energy = 16.3 MeV, the incompressibility K = 240 MeV, symmetry energy S_0 = 31.5 MeV, and the slope L [$\equiv 3\rho_0(\mathrm{d}S(\rho_B)/\mathrm{d}\rho_B)_{\rho_B=\rho_0}$] = (60~70) MeV, taking into account the ambiguity of the empirical value of the L[20]. Also the equations of motion for the meson mean-fields are imposed:

$$\begin{aligned}m_\sigma{}^2\langle\sigma\rangle_0&=\sum_{b=p,n}g_{\sigma b}\left(\rho_b^s+c_3\rho_B^2\bar{I}(p_F(b))\right)\ ,\\m_\omega{}^2\langle\omega_0\rangle_0&=\sum_{b=p,n}g_{\omega b}\rho_b\ .\end{aligned}\tag{9}$$

In addition, the c_3, c_4 and η is determined so as to give the ρ_B-dependence of the energy contribution from the many-nucleon repulsion, E (TNR) (=$\mathcal{E}$(MBR)/ρ_B), similar to that in LP (1981)[19], in particular, being set to the same value at ρ_0 [$E(\mathrm{TNR})_{\rho_0}$=3.52 MeV] as LP (1981).

For the meson-hyperon (Y) coupling constants, the vector meson couplings for Y are obtained from the vector-nucleon couplings $g_{\omega N}$, $g_{\rho N}$, $g_{\phi N}$ through the SU(6) symmetry relations. The scalar (σ, σ^*) meson-hyperon couplings are determined from the phenomenological analyses of recent hypernuclear experiments. The σ-Y coupling constants are obtained so as to reproduce the potential depth of the hyperon Y (= Λ,Ξ^-,Σ^-), V_Y^N, in the SNM. The values of the V_Y^N are set to be V_Λ^N = −27 MeV, $V_{\Sigma^-}^N$ =

23.5 MeV, and $V_{\Xi^-}^N$ = −14 MeV, from which one obtains $g_{\sigma\Lambda}$, $g_{\sigma\Sigma^-}$, and $g_{\sigma\Xi^-}$, respectively. The σ^*-Y coupling constants are simply taken from Refs. [16, 18]. In Table 1, the relevant coupling contants and other parameters are listed. See Ref. [18] for details of obtaining the meson-Y coupling constants.

Table 1　The parameters c_3, c_4, η for the CovMBR3, 4, and γ_a, η_a for TNA, the coupling constants, $g_{\sigma N}$, $g_{\omega N}$, $g_{\rho N}$, the meson mean-fields, $\langle\sigma\rangle_0$, $\langle\omega_0\rangle_0$, and the effective mass ratio for the nucleon, $(M_N^*/M_N)_0$, in the SNM at ρ_0 in the case of L = 70 MeV. The σ-Y coupling constants ($Y = \Lambda, \Sigma^-, \Xi^-$) determined from the potential depths for Y in the SNM are also listed.

c_3/(MeV·fm^{-6})	c_4/(MeV·fm^{-3})	η/fm^6	γ_a/(MeV·fm^{-6})	η_a/fm^3	$g_{\sigma N}$	$g_{\omega N}$	$g_{\rho N}$	$\langle\sigma\rangle_0$/MeV	$\langle\omega_0\rangle_0$/MeV	$(M_N^*/M_N)_0$	$g_{\sigma\Lambda}$	$g_{\sigma\Sigma^-}$	$g_{\sigma\Xi^-}$
0.626	2.50	0.240	−162 2.97	18.52	5.81	9.30	3.35	42.86	18.66	0.73	3.59	2.41	1.94

2　Results

2.1　Energy per particle in SNM

In Fig. 1, the total energy per nucleon, E (total) (= $\mathcal{E}/\rho_{\rm B}$), and each energy contribution are shown as functions of $\rho_{\rm B}$ in SNM (solid lines), obtained by the (MRMF+MBR+TNA) model in the case of the slope L = 70 MeV. E (TNR) [= $\mathcal{E}$ (MBR)/$\rho_{\rm B}$ = ($\mathcal{E}$ (CovMBR3) + $\mathcal{E}$ (CovMBR4))/$\rho_{\rm B}$] is the contribution from many-baryon repulsion coming from mainly three-nucleon-repulsion, E (TNA) [= $\mathcal{E}$(TNA)/$\rho_{\rm B}$] from the three-nucleon attraction, and E (two-body) is the sum of baryon kinetic energy and two-body (meson-B) interaction energy. For comparison, those obtained from LP (1981)[19] are shown by the dashed lines. One can see that the energy contributions from the TNR and TNA, for not only around ρ_0 but also over the relevant densities, are quantitatively close to those in LP (1981). It should be noted that the energy contribution from the CovMBR3 (dot-dashed line) is saturated at higher density $\rho_{\rm B}\sim$ 0.7fm^{-3}, reflecting the density dependence of $\rho_{\rm B}^s$ in the RMF. On the other hand, the one from the CovMBR4 (two-dotted-dashed line) increases with density monotonically and it surpasses the CovMBR3 beyond the density 0.65 fm^{-3}.

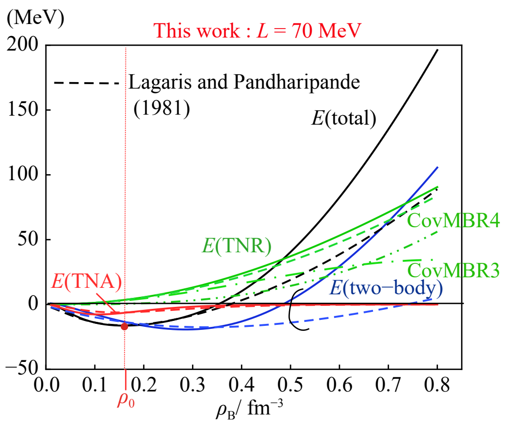

Fig. 1　(color online) The total energy per nucleon, E (total) (= $\mathcal{E}/\rho_{\rm B}$), and each energy contribution as functions of $\rho_{\rm B}$ in SNM (solid lines), obtained by the (MRMF+MBR+TNA) model in the case of the slope L = 70 MeV. For comparison, those obtained from LP (1981)[19] are shown by the dashed lines.

The contribution from the "two-body" interaction, E (two-body), is largely affected by the choice of L through the isospin-dependence of the TNA [the last term in Eq. (5)]. In the case of L = 70 MeV, E (two-body) becomes large at large densities $\gtrsim$ 0.4 fm^{-3}, reflecting the repulsive interaction brought about by the ω-meson exchange between baryons, as compared with the E (two-body) for LP(1981), which is based on the standard variational method. At higher densities $\rho_{\rm B}\gtrsim$ 0.7 fm^{-3}, the two-body contribution to the repulsive energy is comparable to the E (TNR). Therefore the repulsive contribution of E (two-body) is important for stiffening the EOS at high densities as well as E (TNR).

2.2　Bulk properties of neutron stars with the (Y+K) phase and causality condition

The gravitational mass M to radius R relations after solving the Tolman-Oppenheimer-Volkoff equation for L = 70 MeV and Σ_{Kn} = 300 MeV, obtained with the nonlinear chiral effective Lagrangian + MRMF+MBR+TNA model, is shown as the red line in Fig. 2. Some observational ranges for gravitational mass[11, 13] and for gravitational mass and radius from NICER (Neutron star Interior Composition ExploreR)[21−22] are shown. The point at which the (Y+K) phase appears in the center of the core is denoted as a red point. For comparison, those in the previous results are shown, where the universal three-baryon repulsion (UTBR) based on the String Junction Model-2[14−15] (SJM2) is utilized in place of CovMBR3+CovMBR4, for L = (60, 65, 70) MeV and Σ_{Kn} = (300, 400) MeV[17]. The branches including KC in the core are denoted as the black bold solid lines (blue thin solid lines) for Σ_{Kn} = 300 MeV (400 MeV). In addition, the branch with pure Y-mixed matter, where KC is switched off by setting $\theta = 0$, is shown by the green dashed line for each case of L. One can see from Fig. 2 that the present result with L = 70 MeV almost coincides with the previous one with L = 65 MeV. It is due to the fact that enhancement of the s-wave K-B attractive scalar interaction by the introduction of CovMBR3 in Eq. (8) makes up with the difference of repulsion from the two-baryon interaction between the case of L = 70 MeV in the present model and that of L = 65 MeV in the previous model.

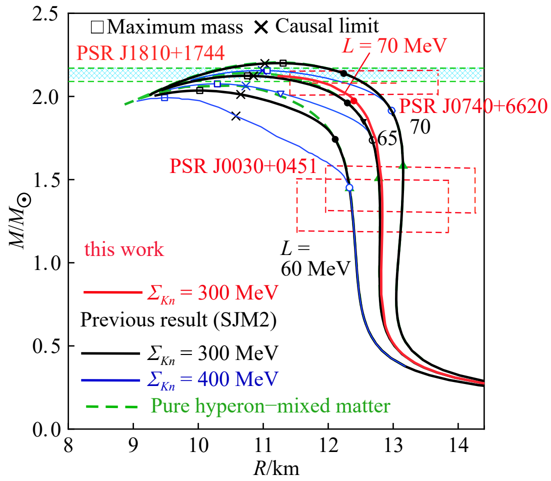

Fig. 2 (color online) The gravitational mass M to radius R relations after solving the Tolman-Oppenheimer-Volkoff equation for L = 70 MeV and Σ_{Kn} = 300 MeV, obtained with MRMF+MBR+TNA (the red line). For comparison, the previous results with the use of String-Junction Model-2[14−15] (SJM2) in place of CovMBR3+CovMBR4 for L = (60, 65, 70) MeV and Σ_{Kn} = (300, 400) MeV[17] are shown by the black or blue solid lines. See the text for details.

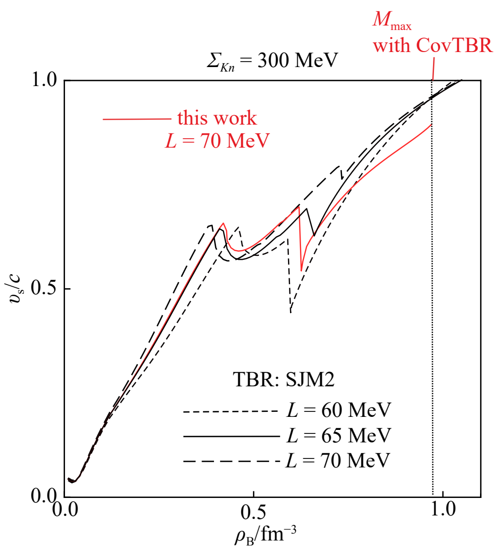

Fig. 3 (color online) Sound velocity $v_s \equiv \left(\frac{dP}{d\mathcal{E}}\right)^{1/2}_{\rm ad.}$ in the unit of the light velocity c as a function of baryon number density $\rho_{\rm B}$ for L = 70 MeV and Σ_{Kn} = 300 MeV (the red line). For comparison, the previous results with the use of String-Junction Model-2[14−15] (SJM2) in place of CovMBR3+CovMBR4 for L = (60, 65, 70) MeV and Σ_{Kn} = 300 MeV[17] are shown by the dotted, solid, and dashed lines, respectively. See the text for details.

In Fig. 3, sound velocity $v_s \equiv \left(\frac{dP}{d\mathcal{E}}\right)^{1/2}_{\rm ad.}$ in the unit of the light velocity c is shown as a function of baryon number density $\rho_{\rm B}$ for L = 70 MeV and Σ_{Kn} = 300 MeV (the red line). For comparison, the ones with the SJM2 model for the UTBR[16] are shown for L = 60 MeV (the dotted line), 65 MeV (the solid line), and 70 MeV (the dashed line). In the present result, the causality condition is fulfilled at least neutron-star mass reaches the maximum mass (= 2.12 $M_\odot$) for L = 70 MeV and Σ_{Kn} = 300 MeV in the present model. In the previous case, the causality condition is fulfilled for a larger value of L, *e.g.* L = 70 MeV until the mass reaches the maximum mass, while it is violated for L = 60 MeV and 65 MeV before the mass reaches the maximum mass[16](see also Fig. 2.). It is to be noted that the Lorentz scalar form of the MBR is necessary but is not sufficient for the fulfillment of causality condition. Indeed the many-baryon repulsion more than two-body force eventually leads to violation of the causality condition for sufficiently high baryon densities. But in this work, the density at the causal limit shifts to a high density beyond the density at the center of compact stars with maximum mass. There are two cusps for every branch in Fig. 3. The lower density one (the higher density one) corresponds to onset of Λ hyperon-mixing (onset of KC), As density increases, the sound velocity v_s in hadronic matter becomes large and approaches the light velocity c due to the repulsive B-B interaction. This result should be compared with the case of hadron-quark crossover[23].

3 Summary and outlook

Lorentz-scalar form of the TBR extended to many baryon forces (Covariant MBR) has been phenomenologically obtained, combined with the nonlinear chiral effective Lagrangian + MRMF+MBR+TNA, in order that the EOS should be consistent with saturation properties of SNM, causality condition, and observations of massive compact stars. In order to be consistent with causality condition, the two-body contribution to the repulsive energy ought to be comparable to the E (TNR) at higher densities $\rho_{\rm B} \gtrsim$ 0.7 fm^{-3}. Otherwise the dominant contribution of E (MBR) over E (two) leads to violation of the causality condition. With the covariant MBR, the EOS including the (Y+K) phase predicts higher L (~70 MeV) in order to obtain bulk properties of neutron stars similar to the previous case with L = 65 MeV by the use of the SJM2 model.

As an outlook, it is suggested from heavy-ion collision experiment that the EOS in SNM or in pure neutron matter may be softer for $\rho_{\rm B}$ =(2~4.5) ρ_0 [24]. Pion condensation (PC), which may be realized at rather low densities $\rho_{\rm B} \gtrsim 2\rho_0$, may have a role as softening mechanisms of the EOS at relevant densities[2]. Possible coexistence of PC and KC (π-K condensation) may be a realistic form of hadronic phase.

With regard to cooling of neutron stars, baryon superfluidity in the presence of KC or π-K condensation is needed to consider on an equal footing as well as neutrino emissivity due to the Kaon-induced Urca process in order to suppress too rapid neutrino emissivities in meson condensates.

In order to clarify the existence of the $(Y+K)$ phase, various new phenomena unique to the $(Y+K)$ phase should be made clear, for example, response to rotation and strong magnetic field of KC as superconductivity, and response of KC to radial/nonradial oscillations of compact stars.

Recently, hadron-quark crossover has been studied extensively to obtain massive compact stars compatible with observations[25–26]. In this context, possible connection of hadronic matter including the $(Y+K)$ phase with quark matter at high densities is indispensable. Unified description of meson condensation in both phases is also an important subject.

References:

[1] KAPLAN D B, NELSON A E. Phys Lett B, 1986, 175: 57.
[2] MUTO T, TAMAGAKI R, TATSUMI T. Prog Theor Phys Suppl, 1993, 112: 159; MUTO T, TAKATSUKA T, TAMAGAKI R, et al. Prog Theor Phys Suppl, 1993, 112: 221.
[3] THORSSON V, PRAKASH M, LATTIMER J M. Nucl Phys A, 1994, 572: 693. Nucl Phys A, 1994, 574: 851.
[4] KOLOMEITSEV E E, VOSKRESENSKY D N, KÄMPFER B. Nucl Phys A, 1995, 588: 889.
[5] LEE C H, BROWN G E, MIN D P, et al. Nucl Phys A, 1995, 585: 401.
[6] GLENDENNING N K, SCHAFFNER-BIELICH J. Phys Rev C, 1999, 60: 025803; GLENDENNING N K. Phys Rep, 2001, 342: 393.
[7] NISHIZAKI S, YAMAMOTO Y, TAKATSUKA T.Prog Theor Phys, 2002, 108: 703.
[8] DEMOREST P B, PENNUCCI T, RANSOM S M, et al. Nature, 2010, 467: 1081.
[9] FONSECA E, PENNUCCI T T, ELLIS J A, et al. Astrophys J, 2016, 832: 167.
[10] ANTONIADIS J, FREIRE P C C, WEX N,et al. Science, 2013, 340: 6131.
[11] CROMARTIE H T, FONSECA E, RANSOM S M, et al. Nat Astron, 2020, 4: 72.
[12] FONSECA E, CROMARTIE H T, PENNUCCI T T, et al. Astrophys J L, 2021, 915: L12. arXiv: 2104.00880.
[13] ROMANI R W, KANDEL D, FILIPPENKO A V, et al. Astrophys J L, 2021, 908: L46.
[14] TAMAGAKI R. Prog Theor Phys, 2008, 119: 965.
[15] TAKATSUKA T, NISHIZAKI S, TAMAGAKI R. AIP Conf Proc, 2008, 1011: 209.
[16] MUTO T, MARUYAMA T, TATSUMI T. Phys Lett B, 2021, 820: 136587.
[17] MUTO T. to be submitted.
[18] MUTO T, MARUYAMA T, TATSUMI T. Prog Theor Exp Phys, 2022, 2022: 093D03.
[19] LAGARIS I E, PANDHARIPANDE V R. Nucl Phys A , 1981, 359: 349.
[20] OERTEL M, HEMPEL M, KÄHN T, et al. Rev Mod Phys, 2017, 89: 015007.
[21] RILEY T E, WATTS A L, BOGDANOV S, et al. Astrophys J, 2019, 887: L21.
[22] MILLER M C, LAMB F K, DITTMANN A J, et al. Astrophys J, 2019, 887: L24.
[23] KOJO T. Phys Rev D, 2021, 104: 074005.
[24] DANIELEWICZ P, LACEY R, LYNCH W G. Science, 2002, 298: 592.
[25] MASUDA K, HATSUDA T, TAKATSUKA T. Astrophys J, 2013, 764: 12; PTEP, 2016. 2: 021D01.
[26] BAYM G, HATSUDA T, KOJO T, et al. Rept Prog Phys, 2018, 81: 056902.

因果率限制下重子三体力对K介子凝聚状态方程的影响

武藤巧[1)]

(千叶工业大学物理系，日本 千叶 275-0023)

摘要: 考虑超子混合物质中存在K介子凝聚相的可能性，此类高密度多奇异系统可能存在于中子星内部。具体来说，基于K介子-重子和K介子-K介子相互作用的手征对称性，结合了二体重子-重子（B-B）相互作用的相对论平均场理论，本工作发展了相互作用模型，其中唯象引入了多重子排斥力（MBR）和三核子引力（TNA）的洛伦兹不变形式，而相关的参数由对称核物质的饱和性质和声速小于光速的因果率进行约束。结果表明，在超子混合物质中具有K介子凝聚的状态方程足够硬，其预言的中子星质量与最近对大质量中子星的观测结果一致。

关键词: 致密强子物质；K介子凝聚；状态方程；因果关系

收稿日期: 2023-12-12；　**修改日期:** 2024-03-18

1) E-mail: takumi.muto@it-chiba.ac.jp